



Comparative assessment of microplastics in water and sediment of a large European river

Christian Scherer^{a,b,*}, Annkatrin Weber^a, Friederike Stock^b, Sebastijan Vurusic^a, Harun Egerci^a, Christian Kochleus^b, Niklas Arendt^b, Corinna Foeldi^c, Georg Dierkes^c, Martin Wagner^d, Nicole Brennholt^b, Georg Reifferscheid^b

^a Goethe University Frankfurt am Main, Department Aquatic Ecotoxicology, Faculty of Biological Sciences, Max-von-Laue-Str. 13, 60438 Frankfurt am Main, Germany

^b Federal Institute of Hydrology, Department Biochemistry, Ecotoxicology, Am Mainzer Tor 1, 56068 Koblenz, Germany

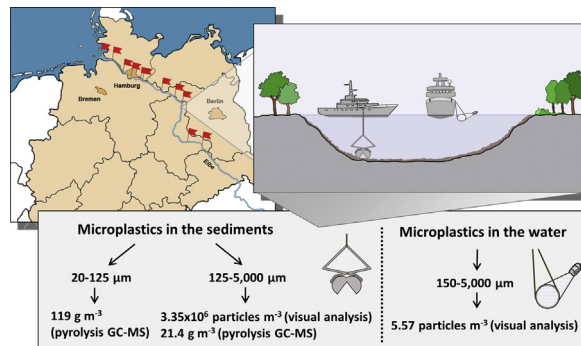
^c Federal Institute of Hydrology, Department Aquatic Chemistry, Am Mainzer Tor 1, 56068 Koblenz, Germany

^d Norwegian University of Science and Technology, Department of Biology, Høgskoleringen 5, 7491 Trondheim, Norway

HIGHLIGHTS

- Low to medium microplastic (MP) levels in the river Elbe
- Much higher MP abundance in sediments compared to the water phase
- Decreasing levels of MP in sediments over the course of the river
- Higher polymer diversity in sediments compared to the water phase
- Industrial emissions possibly caused MP hotspots

GRAPHICAL ABSTRACT



ARTICLE INFO

Article history:

Received 9 April 2020

Received in revised form 29 May 2020

Accepted 30 May 2020

Available online 2 June 2020

Editor: Damia Barcelo

Keywords:

Plastic polymers

Abundance

Visual analysis

Pyrolysis GC-MS

ATR-FTIR

Freshwater

ABSTRACT

Aquatic ecosystems are globally contaminated with microplastics (MP). However, comparative data on MP levels in freshwater systems is still scarce. Therefore, the aim of this study is to quantify MP abundance in water and sediment of the German river Elbe using visual, spectroscopic (Fourier-transform infrared spectroscopy) and thermo analytical (pyrolysis gas chromatography mass spectrometry) methods. Samples from eleven German sites along the German part of the Elbe were collected, both in the water and sediment phase, in order to better understand MP sinks and transport mechanisms. MP concentrations differed between the water and sediment phase. Sediment concentrations (mean: 3,350,000 particles m^{-3} , 125–5000 μm MP) were in average 600,000-fold higher than water concentrations (mean: 5.57 particles m^{-3} , 150–5000 μm MP). The abundance varied between the sampling sites: In sediments, the abundance decreased in the course of the river while in water samples no such clear trend was observed. This may be explained by a barrage retaining sediments and limiting tidal influence in the upstream parts of the river. Particle shape differed site-specifically with one site having exceptionally high quantities of spheres, most probably due to industrial emissions of PS-DVB resin beads. Suspended MP consisted predominantly of polyethylene and polypropylene whereas sediments contained a higher diversity of polymer types. Determined MP concentrations correspond well to previous results from other European rivers. In a global context, MP levels in the Elbe relate to the lower (water) to middle

* Corresponding author at: Federal Institute of Hydrology, Department Biochemistry, Ecotoxicology, Am Mainzer Tor 1, 56068 Koblenz, Germany.
E-mail address: scherer@bafg.de (C. Scherer).

section (sediment) of the global range of MP concentrations determined for rivers worldwide. This highlights that elevated MP levels are not only found in single countries or continents, but that MP pollution is an issue of global concern.

© 2020 The Authors. Published by Elsevier B.V. This is an open access article under the CC BY license (<http://creativecommons.org/licenses/by/4.0/>).

1. Introduction

Microplastics (MPs) have been investigated for over 45 years especially in the marine environment (Bergmann et al., 2015; Carpenter et al., 1972; Cole et al., 2011), but only in recent years research has also started to focus on freshwater environments (Dris et al., 2015b; Wagner and Lambert, 2018). With regard to European rivers, previous studies have investigated MPs in the catchments of the rivers Rhine (Heß et al., 2018; Klein et al., 2015; Leslie et al., 2017; Mani et al., 2015, 2019), Danube (Heß et al., 2018; Lechner et al., 2014), Weser (Heß et al., 2018), Antuã (Rodrigues et al., 2018), Meuse (Leslie et al., 2017), Seine (Dris et al., 2015a), Rhône (Faure et al., 2015) as well as smaller rivers and tributaries in the United Kingdom (Blair et al., 2019; Horton et al., 2017; Hurley et al., 2018; Tibbetts et al., 2018). Furthermore, Leslie et al. (2017) and Schmidt et al. (2018) published first data on MP contamination in canals of large European cities (Amsterdam, Berlin).

In recent publications, reported MP concentrations in European river water varied distinctively ranging from 0.03 (Mani et al., 2019) to 187,000 particles (p) m⁻³ (Leslie et al., 2017). MPs in river water also obtained a broad range of shapes including spheres, fibres, fragments and foils with varying relative abundances. In the Rhine and the Danube, Heß et al. (2018) mostly detected fibres and fragments in the water phase, while Mani et al. (2015, 2019) and Lechner et al. (2014) predominantly found MP spheres. In regard to MP polymer types, polyethylene (PE), polypropylene (PP) and polystyrene (PS) predominated in the river water (Heß et al., 2018; Mani et al., 2015, 2019; Schmidt et al., 2018).

In European river sediments, reported MP concentrations ranged between 18 (Rodrigues et al., 2018) and 72,400 p kg⁻¹ sediment (Hurley et al., 2018) with fragments, fibres and spheres being most abundant (Blair et al., 2019; Horton et al., 2017; Hurley et al., 2018; Klein et al., 2015; Leslie et al., 2017; Rodrigues et al., 2018; Tibbetts et al., 2018). Polymer type composition in the sediments was more diverse than in the water comprising polymer types such PE, PP and PS, but also polyvinyl chloride (PVC), polymethyl methacrylate (PMMA) and dye particles (Horton et al., 2017; Klein et al., 2015; Tibbetts et al., 2018).

MP pollution, both in the water and sediments of European rivers, has been related to multiple pollution sources. Urbanization has been discussed as one major cause of MP pollution in European rivers (Mani et al., 2015; Schmidt et al., 2018; Tibbetts et al., 2018), including pollution both from industry (Mani et al., 2015) as well as land run-offs (Horton et al., 2017). Further, Heß et al. (2018) pointed out that small and medium-sized rather than large rivers obtain high MP levels. Inflowing tributaries and rivers could thus be a relevant MP source for larger rivers (Klein et al., 2015). Wastewater treatment plants (WWTP) are another relevant MP source, although the extent of their importance needs further clarification (Mani et al., 2015; Leslie et al., 2017; Schmidt et al., 2018). Finally, also meteorological and hydrodynamic events may strongly impact MP levels in European river systems (Hurley et al., 2018; Schmidt et al., 2018).

These previous results demonstrate well that MP is an abundant pollutant in freshwater systems across Europe. However, despite the relatively large number of publications, it remains difficult to draw conclusions on the MP distribution in European rivers as most studies investigated MPs only in one specific compartment, that is the riverbed, the water phase or the shoreline. Only two studies included data on MP concentrations both in the water and the sediment phase (Leslie et al., 2017; Rodrigues et al., 2018). However, in these studies MP

concentrations were reported using incomparable units that hamper a direct comparison of MP levels in riverine water and sediment. Further, none of the two studies reported compartment-specific data on MP polymer type distributions.

We approached this knowledge gap by analysing the spatial distribution of MPs in the water and sediment phase in the German part of the large European river Elbe. We chose to study the Elbe as it is an important German waterway with industrial zones and large cities such as Hamburg. Our data, thus, adds to the knowledge on MP concentrations in large European rivers. Water and sediment samples were taken at eleven sites along the river course from the Middle Elbe to its estuary. We analysed MPs in the water (150–5000 µm) and the sediment phase (20–5000 µm) using visual identification as well as analytical verification with pyrolysis gas chromatography coupled to mass spectrometry (pyr-GC-MS) and attenuated total reflection Fourier-transform infrared spectroscopy (ATR-FTIR). To enable a comparison between compartments and with previous studies, we provided results in several units.

2. Materials and methods

2.1. Study site

The Elbe is a 1091 km long river with its source in the Giant Mountains in the Czech Republic. From there, it passes through eastern and northern Germany, before it discharges into the North Sea. The Elbe obtains a total catchment area of 148,268 km² with 96,932 km² located on German state territory. The Elbe is separated into the Upper Elbe (source to Castle Hirschstein, river km 369.92–96 (km 369.92–0 being located on Czech state territory, km 0–96 km on German state territory), the Middle Elbe (Castle Hirschstein to barrage at Geesthacht, river km 96–585.9) and the Lower Elbe (barrage at Geesthacht to the border of the North Sea at Cuxhaven-Kugelbake, river km 585.9–727.7, Naumann et al., 2003). The most important tributaries of the Elbe river are the Moldau (Czech Republic), Saale, Havel and Mulde (Germany). Saale and Havel contribute a water volume of in average 115 m³ s⁻¹ and the Mulde of 73 m³ s⁻¹ to the mean discharge of the Elbe.

In total, eleven sites along the German part of the Elbe were sampled (Table 1, Fig. 1). The sampling sites Wittenberg, Dessau, Havelberg, Wittenberge and Dömitz stretch along the Middle Elbe from km 216 to 516. At Geesthacht (km 585.9), a barrage separates the Middle from the Lower Elbe (the sampling site Geesthacht is

Table 1
Geographical information about the Elbe sampling sites.

Site (abbreviation)	Elbe km	Geo-Longitude	Geo-Latitude
Wittenberg (WB)	216.4	12.6151 E	51.8629 N
Dessau (DS)	261.4	12.2191 E	51.8563 N
Havelberg (HB)	422	12.0766 E	52.8234 N
Wittenberge (WE)	454.9	11.7456 E	52.9904 N
Dömitz (DM)	507	11.2091 E	53.1443 N
Geesthacht (GH)	584.5	10.3586 E	53.4297 N
Elbstorf (ET)	589	10.2909 E	53.4261 N
Hafenstraße (HS)	623.5	10.0391 E	53.5290 N
Lüthemündung (LM)	645.5	9.6350 E	53.5727 N
Hollerwetteren (HW)	681.4	9.3487 E	53.8270 N
Vogelsand (VS)	746.3	8.4876 E	53.9670 N

located upstream of the barrage). Further downstream, Elbstorf, Hafenstraße, Lühemündung and Hollerwetteren are located from Elbe km 589 to 681. Hafenstraße was the most urban sampling site being located in the centre of Hamburg harbour. The site Vogelsand is part of the Outer Elbe, the continuation of the estuary formed by the North Sea.

2.2. Sampling

The sampling was conducted during a routine monitoring of the Elbe by the German Federal Institute of Hydrology (Middle Elbe: 20/07–23/07/2015, Lower and Outer Elbe: 03/08–06/08/2015). Mean flow rates at the sites Wittenberg (km 214) and Wittenberge (km 453) during sampling were relatively low equalling $119\text{--}128\text{ m}^3\text{ s}^{-1}$ and $247\text{--}260\text{ m}^3\text{ s}^{-1}$, respectively. All samples in the Middle and Lower Elbe were taken either at the entrance of harbours or at the edge of the river where fine-grained sediment accumulates.

Ten water samples (one sample per site, except for site Elbstorf where only sediment was collected) were retrieved with an Apstein plankton net (opening: 0.022 m^2 , $\varnothing 17\text{ cm}$, length: 110 cm , mesh size: $150\text{ }\mu\text{m}$) fixed on the side of a research vessel. The plankton net was placed directly below the water surface. The river surface was sampled over a distance of approximately 1 km at a speed of about $6\text{--}7\text{ km h}^{-1}$. The filtered water volume was calculated using a manual flowmeter (fixed on the plankton net opening) and following formula: Filtered water volume = number of flowmeter revolutions $\times 0.3\text{ m revolution}^{-1} \times$ opening of the net [m^2] $\times 1000$. Depending on the flow velocity, $3.2\text{--}32.7\text{ m}^3$ of water were filtered during $5\text{--}10\text{ min}$ (site-specific results in Table S1). The water samples were transferred from the cod end of the net into glass jars via flushing with ultrapure water. After each sampling, the nets were cleaned with ultrapure water to prevent contamination of the subsequent sample.

At the riverbed margins, sediment samples were taken with a Van-Veen-grab sampler ($2\text{--}4\text{ kg}$ per sample). The sediments were stored in closed polypropylene buckets to protect them from external particle contamination.

2.3. Sample preparation

2.3.1. MP extraction from water samples

Water samples were transferred to the Federal Institute of Hydrology and processed as described by Ehlers et al. (2019). In brief, organic matter was digested by adding $5\text{--}15\text{ mL}$ of a $1:1$ mixture of 10 M potassium hydroxide solution and hydrogen peroxide (30%) to each sample. After agitation for $3\text{--}4$ days (d), the samples were neutralized with formic acid. Then, the MP particles were isolated from the remaining matrix in a separating funnel by adding 3.61 g potassium formate powder mL^{-1} sample (density: 1.6 g mL^{-1}). After $3\text{--}4$ d, the uppermost layer of the water phase was separated and pressure-filtrated on anopore inorganic membrane filters (GE Healthcare Life Sciences, Whatman, Anodisc Cat. No. 514–0518, diameter: 47 mm , pore size: $0.2\text{ }\mu\text{m}$). The filters were closed, air dried at $40\text{ }^\circ\text{C}$ and stored in an aluminium jar. Later, filters were visually inspected and all particles $>500\text{ }\mu\text{m}$ as well as selected smaller ones were analysed by means of ATR-FTIR (see Sections 2.4.1, 2.4.2).

2.3.2. MP extraction from sediment samples

Sediment samples were transferred to the Goethe University Frankfurt am Main. For each sampling site, we homogenised the sediment sample first and weighed in up to 2.5 kg of sediment wet weight (ww) afterwards. The dry weight of each sediment sample was determined by drying and weighing a subsample of 200 g ww for $5\text{--}7\text{ d}$ at $45\text{ }^\circ\text{C}$ (results in Table S1).

The sediments ($\leq 2.5\text{ kg}$) were wet-sieved into three size fractions ($20\text{--}125\text{ }\mu\text{m}$, $125\text{--}1000\text{ }\mu\text{m}$, $>1000\text{ }\mu\text{m}$). The $>1000\text{ }\mu\text{m}$ fractions were directly visually sorted and particles with a size of $1000\text{--}5000\text{ }\mu\text{m}$

were stored for further visual and ATR-FTIR analysis. The $20\text{--}125\text{ }\mu\text{m}$ sediment fractions were dried at $45\text{--}55\text{ }^\circ\text{C}$ for $5\text{--}7\text{ d}$ to determine their dry weight (results in Table S1) and afterwards stored in glass jars for pyr-GC-MS analysis. For the sampling sites Dessau, Geesthacht and Elbstorf, we had to wet-sieve two subsamples each, because we lost the $20\text{--}125\text{ }\mu\text{m}$ sediment fractions in the first wet-sieving run and could thus only isolate the $125\text{--}5000\text{ }\mu\text{m}$ fraction. We therefore performed a second wet-sieving run to also obtain the $20\text{--}125\text{ }\mu\text{m}$ sediment fraction from both sites (see Table S1).

The $125\text{--}1000\text{ }\mu\text{m}$ sediment fractions were processed as following. First, density separation was performed in a custom-made replica of the Munich Plastic Sediment Separator (MPSS, Imhof et al., 2012, details in S.1.2) filled with ZnCl_2 ($\rho = 1.6\text{--}1.8\text{ g cm}^{-3}$) as separation solution. A 24 h treatment in the MPSS enabled the isolation of particles with $\rho < 1.6\text{ g cm}^{-3}$. Secondly, the organic content in the isolated particle fraction was further reduced by wet peroxidation ($10:1$ mixture of $30\%\text{ H}_2\text{O}_2$ and $10\%\text{ H}_2\text{SO}_4$, 5 d , $55\text{ }^\circ\text{C}$, details in S.1.2). Finally, the suspensions were filtered on glass microfiber filters (GE Healthcare Life Sciences, Whatman, GF/D, Cat. No. 1823-047, diameter: 47 mm , pore size: $2.7\text{ }\mu\text{m}$) for visual and ATR-FTIR analysis.

2.4. Identification of MPs in water and sediment samples

2.4.1. Visual identification

Tentative MPs on the filters were visually inspected with a (stereo) microscope with attached digital camera (for water samples: Keyence VHX2000, for sediment samples: Olympus SZ-40 and camera (JVC, KY-F75U, imaging software: Discus, version 4.80.8238)). For particle identification, we followed the established criteria by Norén (2007). Tentative MP particles were characterised with regard to their colour (black, white, transparent, grey, silver, brown, purple, blue, turquoise, green, yellow, orange, pink, red), size (longest particle diameter) and shape (fragment, sphere, fibre, foils). Based on the mesh size of the plankton net as well as the sieves used for the wet-sieving of the sediments, $150\text{--}5000\text{ }\mu\text{m}$ (water samples) and $125\text{--}5000\text{ }\mu\text{m}$ (sediment samples) particles were analysed on the filters.

Total particle concentrations in the water phase of each site were calculated based on the filtered water volume and reported as MP number m^{-3} water. Concentrations in sediments are given as MP number m^{-3} dry sediment to allow comparison between water and sediment samples. Sediment volumes were calculated from sediment dry weights and corresponding sediment densities (details in Table S1 and S1.3). We added results on MP concentrations in sediments based on total sediment mass (MP kg^{-1} dry weight) in chapter S2.2.1.

2.4.2. ATR-FTIR analysis

A subsample of the tentative MPs was manually isolated and analysed by ATR-FTIR (Perkin Elmer, Spectrum Two) to determine the polymer type. The majority of the analysed particles were $>500\text{ }\mu\text{m}$. Due to lower MP abundance in the water phase, we could analyse all MP particles $> 500\text{ }\mu\text{m}$ in the water samples, while for the sediment samples only a subsample could be processed. Particle spectra were compared to a self-established plastic polymer data bank with reference spectra for the most common polymer types (PE, PP, PS, PVC, PMMA, polyethylene terephthalate (PET), acrylonitrile butadiene styrene (ABS), polyamide (PA), polyurethane (PU)) and categorised as “MP” (match $>80\%$ and/or clear match of characteristic peaks) or “unknown” (correlation $< 80\%$ and no match of characteristic peaks). For details of ATR-FTIR analysis see S1.4.

2.4.3. Pyrolysis GC-MS analysis

After the removal of large tentative MPs from the filters for ATR-FTIR analysis, we determined the remaining PE, PP and PS content on the filters (originating from 125 to $5000\text{ }\mu\text{m}$ particles) as well as in the fine sediment fraction ($20\text{--}125\text{ }\mu\text{m}$) from the sediment samples via pyr-

GC–MS. We also analysed the filters of the water samples. However, we observed strong interferences in the mass spectra caused by the anodic filters and did not proceed with the analysis.

For pyr-GC–MS, the glass microfibre filters and the fine sediment fractions were separately ground in a laboratory ball mill. However, the powders of the ground filters were too acidic (due to previous wet peroxidation throughout the extraction of the 125–5000 μm sediment fraction, see Section 2.3.2) to be directly used for pyr-GC–MS analysis. Thus, we re-suspended the powder in water, allowed particles to settle (to impede rapid filter blocking) and filtered the majority of the supernatant volume through a glass fibre filter (pore size: 2.7 μm), before adding new water to the ground filter powders. This “washing process” was repeated at least twice (until the washing water had pH 7). Finally, the suspended filter powder was completely transferred on the new filter and dried for 7 d at 55 °C, before milling in a ball mill again.

Polymer extraction and pyr-GC–MS analyses were performed as previously described (Dierkes et al., 2019). In brief, the ground filters with the 125–5000 μm MP particles as well as the fine sediments were pre-extracted with methanol followed by an extraction with tetrahydrofuran using 10 mL extraction cells and an ASE-350 (Dionex, Sunnyvale, CA, USA). The extracts were transferred on calcined silica gel. After the addition of an internal standard (polystyrene- d_5), the calcined silica gel with the adsorbed extracts were analysed by pyr-GC–MS analysis. We monitored for PE, PP and PS based on characteristic pyrolysis products. Polymer abundance was calculated by comparison of the peak intensity of the characteristic pyrolysis products with the results of a calibration standard curve (for further details on pyr-GC–MS analysis, see S1.5).

2.5. Validation and quality control

2.5.1. Validation of MP extraction from water samples

We analysed potential effects of chemical digestion on MP integrity by exposing PE, PET, PP, PS und PVC MPs for 24 h to H_2O_2 (30%) and KOH (10 M). All particles were visually inspected afterwards. MP particles showed almost no signs of degradation.

2.5.2. Validation of MP extraction from sediment samples

The methodology for wet-sieving, density separation and acid digestion (125–1000 μm sediment fraction) was pre-validated threefold using artificial sediments spiked with MP. 1500 g of quartz sand were spiked with 125 MP particles (125–1000 μm) made of PE, PP, PS, PMMA and PVC (25 particles each). The total recovery rate for the whole process equals $87.2 \pm 4.5\%$ (mean \pm SD). The reported MP concentrations may therefore be underestimates of actual concentrations in the sediment samples.

Further, we tested the impact of acid digestion on MP integrity. For this, MPs (473–1385 μm) made of PE, PS, PP, PA and PVC (ten particles each) were incubated in 33 mL of the 10:1 mixture of 30% H_2O_2 and 10% H_2SO_4 for 5 d at 55 °C. Recovery rates were determined both with regard to particle abundance and total surface area. Throughout the acid digestion, no particles were lost and changes in MP particle surface area were minor ($\leq 4.4\%$ surface area reduction) proving limited impacts of the acid digestion methodology on particle integrity.

2.5.3. Controls for water samples

For the extraction process, three “processing blanks” were run by digesting and filtrating 10 mL of distilled water in the same way as the water samples. For quantification of atmospheric fallout, we placed aluminium oxide filters (“sorting blanks”) next to the digital microscope for 12 h (time needed for visual analysis of filters of one sampling site). MPs on the processing and sorting filters were characterised visually. Total MP concentrations in the water samples were corrected for the average particle number on the processing and the sorting blanks, respectively (results in S2.1.1).

2.5.4. Controls for the sediment samples

As for water samples, we included blanks for the extraction process (“processing blanks”) and the visual sorting (“sorting blanks”). Contamination throughout the extraction process was quantified thrice by processing 500 mL distilled water in the same way as the 125–1000 μm sediment fraction (Section 2.3.2). During visual analysis of the samples, we placed empty glass fibre filters next to the stereo microscope to account for atmospheric fallout (one “sorting blank” per sampling site). MPs on the blanks were characterised visually and total MP numbers in the sediment samples were corrected for the average particle number on the processing blank as well as the sample site-specific sorting blank filters (results in S2.1.2 and Table S3).

2.5.5. Controls for the pyrolysis GC–MS

Controls for the pyr-GC–MS methodology were performed multifold by running the pre-extraction and the pyr-GC–MS analysis procedure (see Section 2.4.3) with tempered sea sand (ChemSolute, No. 804.9025) which had been calcined at 600 °C. None of the control runs detected any of the monitored pyrolysis products.

In regard to the filters from the extraction of the 125–5000 μm sediment fraction, we further corrected the pyr-GC–MS results for the contamination throughout the extraction (“processing blanks”) and visual sorting (“sorting blanks”, see Section 2.5.4) of the 125–5000 μm sediment fraction. For this, we determined PE, PP and PS polymer mass concentrations on the “processing” and “sorting blank” filters via pyr-GC–MS (using the same methodology as described in Section 2.4.3) and corrected the mass concentrations of the different sampling sites for the mass concentrations on the blank filters, respectively.

2.6. Statistics

Results were analysed and plotted with GraphPad Prism 7.04 (GraphPad Software Inc., USA). Tentative MP concentrations in water and sediments from the Middle and Lower Elbe were compared with a non-paired, two-tailed *t*-test. Particle size distributions were fitted with a One-phase decay function and a bin width of 200 μm (first bin centre: 250 μm). Further, results from visual MP analysis and pyr-GC–MS were compared with a Spearman correlation.

3. Results

3.1. Numerical concentrations of MPs in Elbe water and sediments

According to the visual analysis of the 125–5000 μm particle fraction, Elbe water samples contained on average 5.57 ± 4.33 (SD) tentative MP particles m^{-3} (p m^{-3} , median: 5.11 p m^{-3}) with concentrations ranging from 0.88 (Geesthacht) to 13.24 p m^{-3} (Dömitz, Fig. 1). The concentration of tentative MPs in sediments was on average 600,000-fold higher (when referring to the same volume). Elbe sediments contained on average $3.35 \times 10^6 \pm 6.60 \times 10^6 \text{ p m}^{-3}$ sediment (median concentration: $7.6 \times 10^5 \text{ p m}^{-3}$; $2.08 \times 10^3 \pm 4.67 \times 10^3 \text{ p kg}^{-1}$ sediment) and ranged from 2.26×10^4 (Vogelsand) to $2.27 \times 10^7 \text{ p m}^{-3}$ (Dessau, Fig. 1).

In regard to MPs in the water phase in the Middle Elbe, highest MP concentrations were recorded at the Dessau site (11.56 p m^{-3}) and at Dömitz (13.24 p m^{-3}). The mean MP concentrations in the water phase in the Lower and Outer Elbe (Hafenstraße to Vogelsand, $3.07 \pm 2.39 \text{ p m}^{-3}$) were lower compared to the Middle Elbe (Wittenberg to Geesthacht, $7.24 \pm 4.68 \text{ p m}^{-3}$). However, the difference was not statistically significant (non-paired, two-tailed *t*-test, $p > 0.05$). Interestingly, MP concentration at Hafenstraße (4.73 p m^{-3}), the site directly located in the city of Hamburg, was lower compared to almost all sites in the Middle Elbe (except for Havelberg), while it was the second highest along the course of the Lower Elbe.

Besides Dessau, sediments from Dömitz contained the second highest MP concentrations ($4.87 \times 10^6 \text{ p m}^{-3}$). Similar to the water

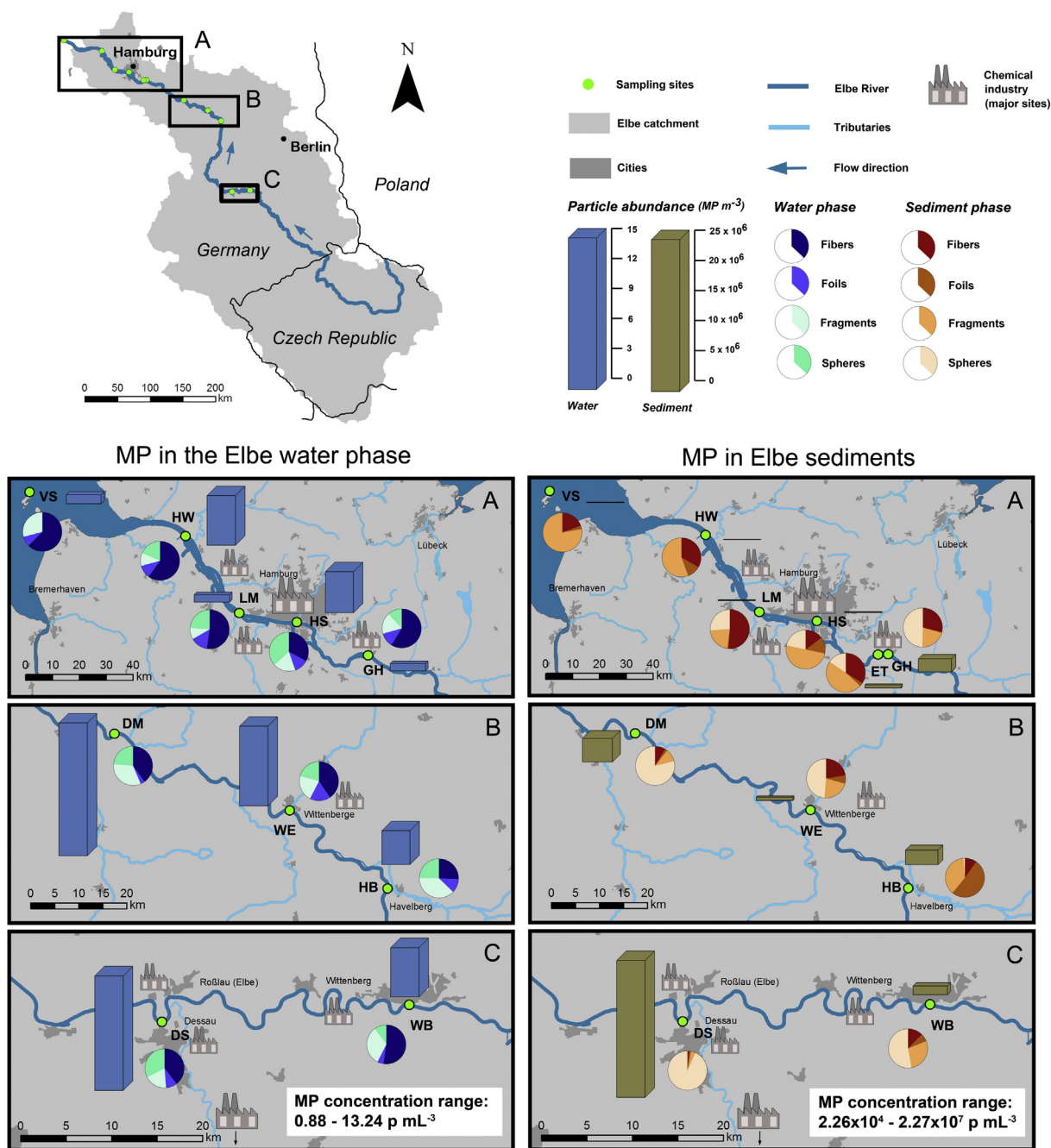


Fig. 1. Concentrations and shape of tentative MPs in water (150–5000 μm particle fraction) and sediment samples (125–5000 μm particle fraction) from eleven sampling sites along the Elbe river. Bars (water: blue, sediment: brown) indicate concentrations (p mL^{-3} water/sediment, note the different scales) and pie charts indicate the relative particle shape distribution (fibres, fragments, spheres, foils). Site abbreviations: WB: Wittenberg, DS: Dessau, HB: Havelberg, WE: Wittenberge, DM: Dömitz, GH: Geesthacht, ET: Elbstorf, HS: Hafenstraße, LM: Lühhemündung, HW: Hollerwettern, VS: Vogelsand.

samples, concentrations in the Lower and Outer Elbe (Elbstorf to Vogelsand, $1.84 \times 10^5 \pm 2.32 \times 10^5 \text{ p mL}^{-3}$) were lower compared to the Middle Elbe (Wittenberg to Geesthacht, $6.0 \times 10^6 \pm 8.29 \times 10^6 \text{ p mL}^{-3}$), but these differences were not significant ($p > 0.05$). Detailed results on numerical concentrations are provided in Table S3.

All four particle shapes (fibre, fragment, sphere, foil) were found both in water and sediment samples (Fig. 1, Fig. S3). On average, water samples mostly contained fibres (46.5%), while fragments (22.9%), spheres (20.1%) and foils (10.6%) were less abundant. In contrast, sediments contained predominantly spheres (35.5%) and fragments (34.2%), whereas only 21.5% and 9.1% of the particles were fibres and foils, respectively. While the particle shape distribution

does not follow a clear trend along the course of the river, notable results were observed at specific sampling sites. At the Dessau site in the Middle Elbe, 93.4% of the MP particles in the sediment were spheres. In the water phase, spheres were less abundant (32.6%) but still the second most common shape following fibres (39.5%). At the river mouth (Hollerwettern, Vogelsand), fibres and fragments were the most abundant MP shapes both in the water and the sediment samples (details in Table S3).

The size distribution of tentative MPs (size range: 125/150–5000 μm) in the water and sediment phase increased exponentially with decreasing particle size (Fig. 2). However, Elbe sediments included a higher proportion of MPs $< 416 \mu\text{m}$ than the samples from the

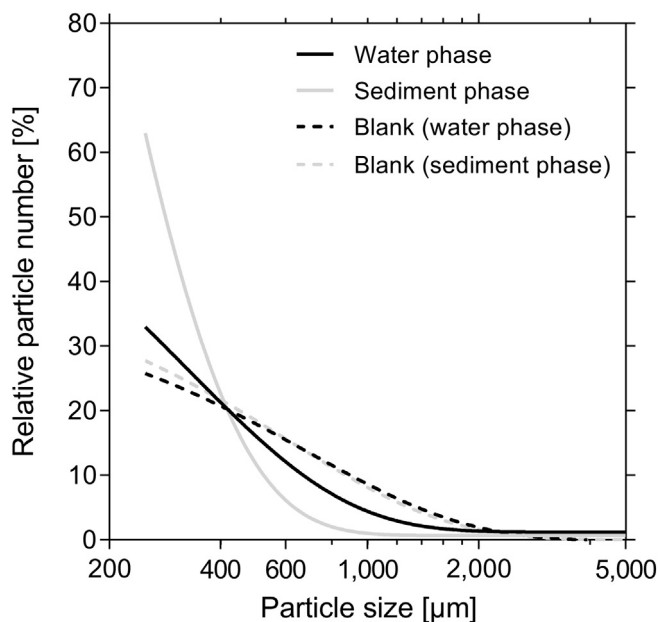


Fig. 2. Average size distributions of tentative MPs in the water and sediment samples from the Elbe river and the corresponding blanks. For better comparability, only particles with a size of 150–5000 μm were included.

water phase (details in Fig. S4). Blanks contained a higher proportion of particles between 500 and 2000 μm .

Tentative MPs in water and sediment samples were mostly transparent (water: 26.0%, sediment: 28.8%), blue (water: 19.7%, sediment: 15.2%) or white (water: 15.0%, sediment: 16.2%, Fig. S5). Furthermore, sediments also contained 10.7% of red MPs. The proportion of transparent and white tentative MP particles in the sediments decreased along the course of the river. At the Dessau site, the high proportion of transparent and white particles (95.5%) is linked to the high concentration of spheres at this sampling site.

3.2. Polymer types of tentative MPs

The polymer type of visually identified MPs in the water and sediment samples was determined by ATR-FTIR (see Section 2.4.2). 41 out

of 584 tentative MPs (7.0%) from the water phase and 269 out of 4965 tentative MPs (5.4%) from sediments were analysed. In the water phase, most particles were made of PE (47.5%) and PP (45.0%), while in the sediments a more diverse set of polymer types was detected (Fig. 3). Besides PE (34.4%) and PP (12.5%), MPs in the sediments were also made of PS (18.5%) as well as ABS, PA, PET and PMMA (in total 2.0%). MP spheres found in very high numbers at the Dessau site were characterised as PS (determined by analysing a subsample of all Dessau spheres; later pyr-GC-MS results indicate that spheres may have actually been made of polystyrene-divinylbenzene (PS-DVB), see Section 4.5). Moreover, the proportion of particles that did not match a plastic type was larger for sediment samples (29.3%) compared to water samples (5.0%).

3.3. Mass-based concentrations of PE, PP and PS in Elbe sediments

3.3.1. Polymer content in the 125–5000 μm fraction of sediments

The mass concentrations of PE, PP and PS in the 125–5000 μm fractions (excluding the MP particles analysed via ATR-FTIR) of the sediment samples were determined by pyr-GC-MS (Fig. 4a, Table S4). In average, Elbe sediments contained 21.4 ± 19.2 g polymer m^{-3} when summing up the PE, PP, PS content that contributed with 75.0, 16.8 and 8.2%, respectively. A marked decrease in concentrations was observed from the sites Wittenberg to Elbstorf compared to the downstream sites Hafenstraße to Vogelsand. Between Wittenberg and Elbstorf, mass concentrations varied intensively with lowest concentrations at the Dessau site (13.7 g m^{-3}) and highest concentrations at Havelberg (49.2 g m^{-3}). From Hafenstraße to the Elbe estuary, the polymer concentrations were much lower, ranging from 1.37 (Vogelsand) to 0.20 g m^{-3} (Lühemündung). When comparing the numerical and mass-based MP concentrations (Fig. 4b), results of both methodologies correlated significantly (Spearman correlation, $p < 0.05$).

3.3.2. Polymer content in the 20–125 μm fraction of sediments

We also determined the PE, PP and PS content in the fine sediment fraction (20–125 μm particles) by pyr-GC-MS and calculated the resulting mass-based polymer concentrations (Fig. 5). On average, sediments contained a total of 119 ± 149 g m^{-3} MPs (PE, PP and PS combined). The highest MP concentrations were found at Elbstorf (482 g m^{-3}) and Geesthacht (317 g m^{-3}). In comparison, the sampling sites Lühemündung (10.6 g m^{-3}), Hollerwetter (15.4 g m^{-3}) and Vogelsand (10.6 g m^{-3}) at the mouth of the Elbe had much lower

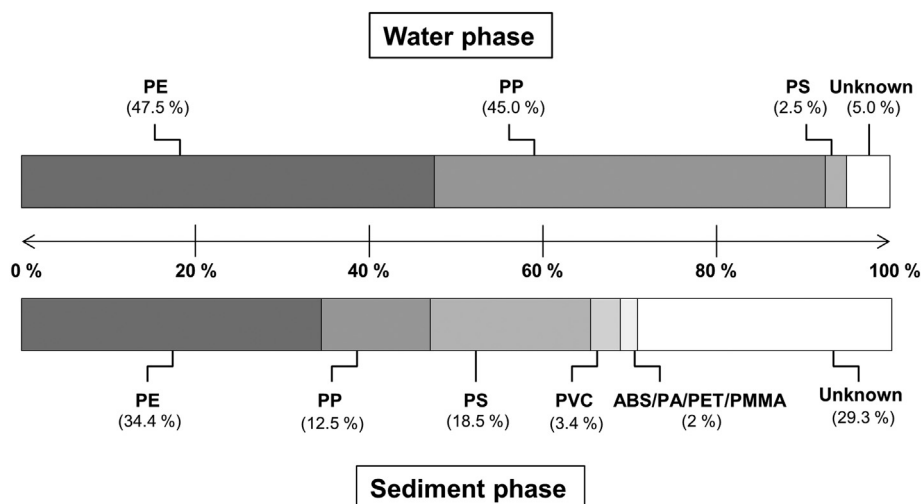


Fig. 3. Average composition of MP polymer types determined by ATR-FTIR analysis in the water and sediment samples from the Elbe river.

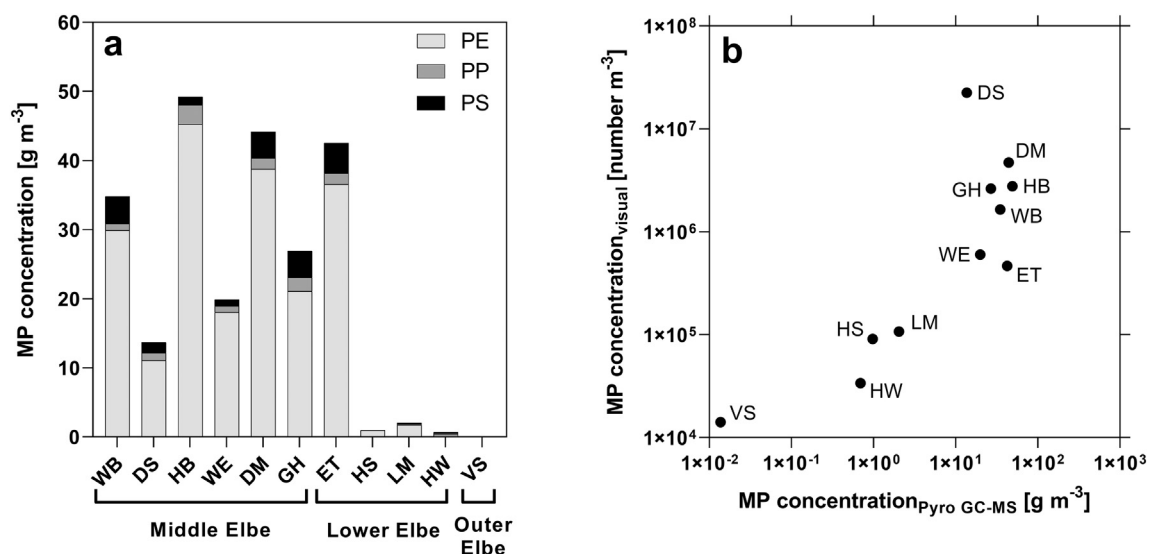


Fig. 4. Mass-based concentrations of the 125–5000 μm fraction of Elbe sediments determined by pyr-GC-MS. (a) Concentrations based on PE, PP and PS content. (b) Comparison of numerical and mass-based MP concentrations. Tentative MP concentrations were corrected for the number of removed particle for ATR-FTIR-analysis as those particles did not contribute to pyr-GC-MS results. For site abbreviations see Fig. 1.

concentrations. Further details on mass concentrations per volume and mass of sediments are provided in Table S5.

PE was the most abundant polymer in the fine sediment fractions at all sites except for Vogelsand. At Elbstorf and Geesthacht, samples contained much higher quantities of PS than PE. When excluding PS, the mean MP concentration was $65.6 \pm 46.4 \text{ g m}^{-3}$, with PE (density: $\sim 0.94 \text{ g cm}^{-3}$) contributing in average 80.94% and PP (density: $\sim 0.91 \text{ g cm}^{-3}$) 19.06% to the polymer mass. Further, mean numerical concentrations were recalculated from the average mass-based concentration. Assuming that all particles are spherical and have an average density of 0.93 g cm^{-3} , MP concentrations range between $8.62 \times 10^3 \text{ p m}^{-3}$ (only 125 μm spheres) and $2.10 \times 10^6 \text{ p m}^{-3}$ (only 20 μm spheres).

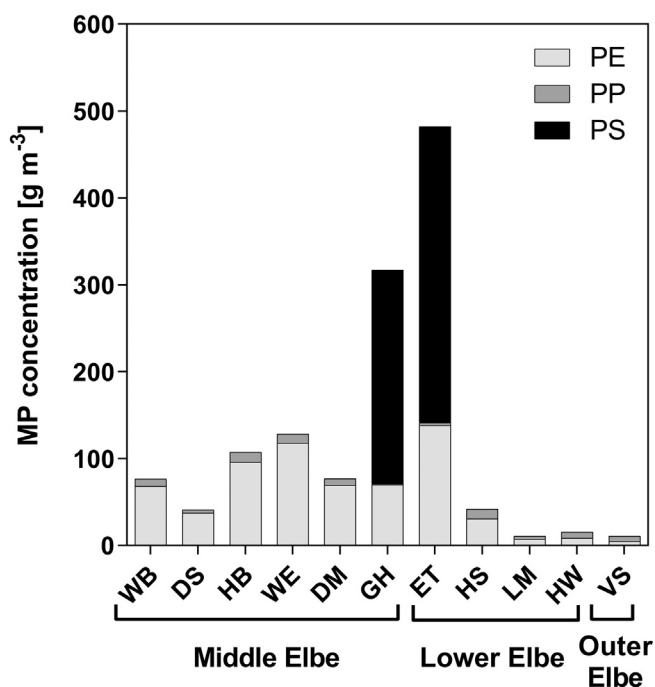


Fig. 5. Mass-based concentrations of the 20–125 μm fraction of Elbe sediments determined by pyr-GC-MS. For site abbreviations see Fig. 1.

4. Discussion

4.1. Riverine sediments are sinks for MPs

MP concentrations (125–5000 μm fraction) in sediments of the river Elbe (2.26×10^4 to $2.27 \times 10^7 \text{ p m}^{-3}$) were in average 600,000-fold higher compared to the water phase (0.88 to 13.24 p m^{-3}). The same tendency is evident on a global scale (Fig. 6, see Section 4.6). In addition, we detected theoretically buoyant PE and PP in the sediments. This is in accordance with previous literature (Klein et al., 2015; Lin et al., 2018; Rodrigues et al., 2018) as weathering and biofouling, inclusions of substances during production, the formation of hetero-aggregates or sorption of biomolecules can increase particle density (Chubarenko et al., 2016; Corcoran, 2015; Moret-Ferguson et al., 2010). River sediments are, therefore, a key sink of MPs.

4.2. MP concentrations tend to decrease in the course of the river

We observed higher MP concentrations in sediments of the Middle Elbe compared to the Lower and Outer Elbe. The sudden decrease in MP concentrations at the sites Elbstorf and Hafenstraße are probably caused by a barrage at Geesthacht which separates the sampling site Geesthacht (Middle Elbe) from the sites in the Lower Elbe (Elbstorf to Hollerwetter). Thus, the tide affects the Outer and Lower Elbe up to the city of Hamburg (Hafenstraße) and to a lower extend up to the site Elbstorf, but not the sites further upstream. Tidal activity leads to a constant exchange of water bodies which may increase the transport of MPs into the North Sea and limit an accumulation of MPs in sediments. Each year, about 625,000 t of fine-grained sediments enter the estuary from the catchment area of the Elbe (IKSE, 2014; Schwartz et al., 2015). The tides also move marine sediments from the North Sea into the estuary (Schwartz et al., 2015) leading to sediment mixture and a further dilution of MP levels. Interestingly, our observations contrast previous publications that reported higher MP concentrations in the estuary compared to the river in the Yangtze and Yellow river (Xiong et al., 2019; Han et al., 2019). Differing results are potentially caused by river morphology and tidal activity as different tidal currents, circulation and geometry of each estuary strongly impact MP transport in lower rivers and estuaries (Wolanski and Elliott, 2015).

In the water phase, MP concentrations were highest in the Middle Elbe and, similar to the sediment phase, also tended to decrease in the course of the river. But in contrast to sediments, concentrations

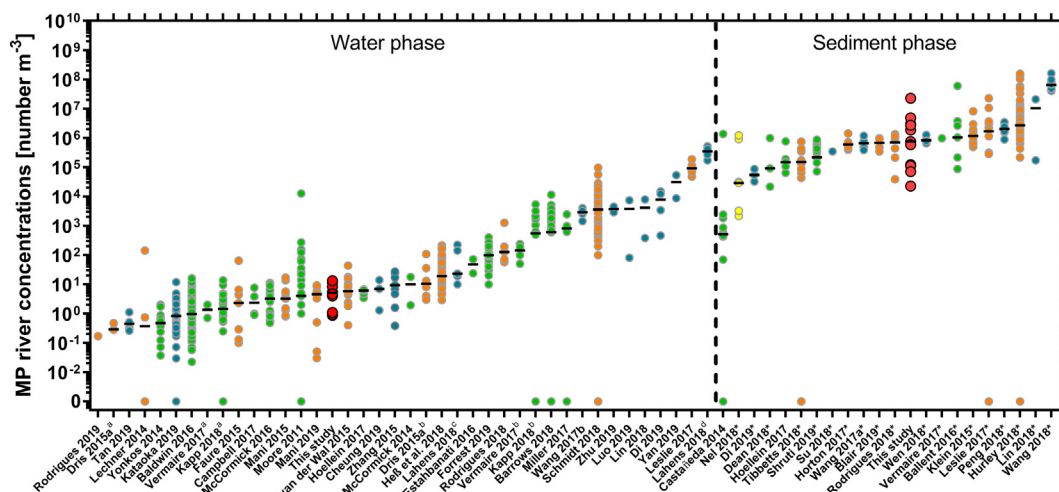


Fig. 6. Summary of published MP concentrations (water and sediment phase, sorted according to median) in rivers in Europe (orange, this study (red)), North- and South America (green), Asia (blue) and Africa (yellow). ^{a,b}For studies using two sampling techniques, we present MP concentrations separately. ^{c,d}Lahens et al. (2018) determined MP concentrations separately for fragments and fibres. ^eStudies reported MP concentrations as p kg^{-1} sediment. Concentrations were recalculated to p m^{-3} sediment based on a density of 2.17 kg dm^{-3} (average density of the eleven Elbe sediments) (e.g., analyzed references are listed in S4).

varied more intensively as higher MP concentrations were also detected in the Lower Elbe, especially at the sites Hafenstraße and Hollerwettern. Thus, tidal activity does not seem to affect MP concentrations in water in the same way as in sediments. Reduced tidal impacts may be explained by the constant drift of MPs downstream (if particles do not settle). Low retention times may lead to higher (short-term) fluctuation in MP concentrations, while tidal impact, instead, remains rather low.

4.3. MP hotspots highlight the relevance of industrial emissions

Very high MP concentrations were determined in the sediments at the Dessau sampling site. Spherical plastic beads, potentially made of PS-DVB (see Section 4.5, Fig. S6, Table S6), contributed most. This observation coincides with findings in the Lower Rhine. Here, Mani et al. (2019) detected PS-DVB spheres which had most probably been used as ion-exchange resin beads (Mani et al., 2019). The spheres collected at the site Dessau potentially originate from industrial areas of Dessau or Bitterfeld close to the sampling site in which plastic-processing industry has been established (Fig. 1). PS-DVB spheres were probably transported via the Mulde river into the Elbe with its confluence being located close to Dessau. Thus, industrial emissions may play a major role for local MP hotspots.

In contrast to primary MPs, the exact origin and entry pathway for secondary MPs remain unknown. For instance, the composition of sampled MPs is heterogeneous and varies without clear trends (Fig. 1, Table S3). However, it is already known that WWTPs contribute to the MP pollution in rivers (Mani et al., 2015; Leslie et al., 2017). In the catchment of the Elbe, >2000 public waste water treatment plants (WWTPs) exist which clean $>1.40 \times 10^9 \text{ m}^3$ water year⁻¹. These are accompanied by industrial WWTPs which clean an additional water volume of $1.42 \times 10^8 \text{ m}^3$ water year⁻¹ (FGG Elbe, 2014). High cleaning and, thus, discharge rates of WWTPs into the Elbe suggest that WWTPs may be an important source of MP pollution in the Elbe. Determining their relative contribution to the detected MP composition at the examined sampling sites, however, lies beyond the scope of this study.

In general, highly populated urban areas are commonly discussed as a key source of MPs (Duis and Coors, 2016; Horton et al., 2017; Rodrigues et al., 2019). For the Elbe catchment, this could not be verified as water and sediment samples from the harbour area of Hamburg

(Hafenstraße) contained lower MP concentrations compared to other more rural areas (e.g., Dömitz). Low levels may be explained by the constant dredging of the harbour areas to remove deposited sediments. Moreover, as discussed above, tidal influence may have transported sediments from Hamburg further downstream into the North Sea, thereby, reducing MP levels in the harbour sediments.

4.4. MP composition in the water and sediment differs

Sediments contained higher proportions of smaller particles compared to the water phase. Furthermore, sediments contained mainly spheres (due to high proportions (93.4%) at Dessau) and fragments, while fibres dominated the water phase. Reduced particle size and high levels of fragments in sediments point towards MP settlement and fragmentation in the sediments. Similarly, Lin et al. (2018) also observed a high proportion of fragments in sediments of the Pearl River (China), most probably due to a lower surface to volume ratio followed by sedimentation of these fragments (Wang et al., 2017b). Thus, fragments seem to be a relevant MP shape in river sediments.

The larger mean particle size of suspended MPs may possibly be caused by the enhanced proportion of fibres. Waldschläger and Schuettrumpf (2019) as well as Khatmullina and Isachenko (2017) confirmed that fibres obtain a relatively low settling velocity in freshwater experiments. The same is true for marine conditions (Bagaev et al., 2017). Low settling velocities and a constant water stream along the river thus possibly prevents fibres from sinking causing enhanced abundances in the river water phase and reduced accumulation in the sediments.

The polymer distribution differed between the water and sediment phase. In the water samples, MP particles were mostly made of PE and PP ($0.85\text{--}0.92 \text{ g cm}^{-3}$). This is in accordance with previous literature. For instance, PE and PP fragments also dominated in Antuã River (Portugal) as well as in a tributary of the Thames River (Rodrigues et al., 2018; Horton et al., 2017). In the sediments, polymer distribution was more diverse and also included PS (and PS-DVB, see Section 4.3), PVC, ABS, PA, PET and PMMA. On the one hand, the distribution pattern reflects the high production volumes of PE and PP (~50% of total demand, PlasticsEurope, 2017). On the other hand, an increased polymer diversity in the sediments is probably related to polymers with higher density that sink and deposit more easily in sediments (Horton et al., 2017).

4.5. Comparison of MP identification methodologies

In this study, visual identification, pyr-GC-MS and ATR-FTIR methods have been used for analysing and identifying MPs. Analysis by ATR-FTIR was mostly limited to particles $>500\ \mu\text{m}$, while smaller particles were mainly analysed visually and by pyr-GC-MS. Visual analysis, although still the most commonly applied methodology for MP identification, is often criticised as inaccurate and subjective with a high potential to misestimate actual MP concentrations (Hidalgo-Ruz et al., 2012; Loeder and Gerdtz, 2015). In comparison, pyr-GC-MS analysis is often considered advantageous compared to visual analysis due to higher analytical sensitivity (Fischer and Scholz-Böttcher, 2019).

To evaluate the quality of both methodologies in regard to MP quantification, we correlated the results for visual and pyr-GC-MS analysis for 125–5000 μm particles in the Elbe sediments. For the correlation, we assumed that the particle size distribution and the polymer distribution were comparable in the different sediment samples. At least for the particle size distribution, this can mostly be confirmed (Fig. S4). A significant correlation of the numerical (visual) and mass-based concentrations (pyr-GC-MS) suggests that methodologies provide consistent results. Thus, relative proportions between MP concentrations at the different sampling sites are sufficiently determined by both methodologies.

However, it remains unclear whether the results from both methods are also comparable in terms of absolute MP levels at the different sampling sites. For instance, at the site Dessau, visual analysis indicated very high MP numbers (especially spheres, see Section 4.3). ATR-FTIR results confirmed that the spheres were mostly made of PS. Pyr-GC-MS analysis, however, could not find high PS mass in the Dessau sediment sample (Fig. 4). A possible explanation for this analytical discrepancy was potentially found in a follow-up sampling at the site Dessau in 2019: Throughout the new sampling, we detected spherical MPs which resembled the spheres detected as part of this study in 2015. A closer comparison of pyr-GC-MS results of the newly sampled MP spheres with PS reference materials revealed that the PS was crosslinked with DVB (Fig. S6, Table S6). The ATR-FTIR analysis performed throughout this study was not able to highlight this difference as the ATR-FTIR reference data base did not include a PS-DVB reference spectrum. PS-DVB particles are commonly used as ion exchange resins (Brady et al., 2017). The cross-linkage of PS with DVB may have thus affected the styrene detection by pyr-GC-MS. As such, the high number of detected PS spheres may not correlate with the PS mass measured in the pyr-GC-MS. A second explanation for low detected PS mass at Dessau may be related to a potential macroporous structure of the spheres. Macroporosity lowers the relative PS mass per particle volume, and thus the detectable PS mass.

In opposite to the 125–5000 μm sediment fraction, high PS contents in the fine sediments (20–125 μm) were only observed at the sampling sites Geesthacht and Elbstorf, but at none of the other sites. Increased PS abundances may originate from enhanced PS polymer fragmentation, but also from styrol-butadien-rubber (SBR) car tyre abrasion or from other polymers containing styrene (e.g., ABS, Eisentraut et al., 2018; Unice et al., 2012). However, the actual source currently remains unknown.

4.6. MP abundance in a global context

Overall, our results coincide well with previously published data from 51 studies on MP concentrations in rivers worldwide (Fig. 6). Here, median global MP concentrations in the water phase and sediments ranged between 0.17 (Rodrigues et al., 2019) and $3.45 \times 10^5\ \text{p m}^{-3}$ (Lahens et al., 2018) and 5.15×10^2 (Castañeda et al., 2014) and $6.49 \times 10^7\ \text{p m}^{-3}$ (Wang et al., 2018), respectively (Fig. 6).

For water, MP levels in the Elbe (median: $5.11\ \text{p m}^{-3}$) are lower compared to other river systems (Fig. 6). In the context of German

ivers, instead, MP concentrations in the Elbe are comparable to those reported for the Rhine, Danube and Weser (median: $3.27\text{--}19.10\ \text{p m}^{-3}$, Heß et al., 2018, Mani et al., 2015). Higher concentrations (median: $3.60 \times 10^3\ \text{p m}^{-3}$) were only found by Schmidt et al. (2018) who sampled an urban canal in Berlin that may not be representative for MP pollution in large rivers. For sediments, the median MP concentration in the Elbe ($7.57 \times 10^5\ \text{p m}^{-3}$) corresponds to the middle section of global distribution (Fig. 6) and are two orders of magnitude lower than in the most contaminated river. In regard to German rivers, Elbe sediment concentrations matched well with concentrations in the rivers Main and Rhine ($1.16 \times 10^6\ \text{p m}^{-3}$, Klein et al., 2015). We, thus, assume that our measured MP concentrations and compositions are quite representative for German rivers.

However, such comparisons are hampered by the diversity of analysis and methods used in monitoring studies (Mai et al., 2018; Prata et al., 2019). For instance, MP concentrations are based either on numbers or weight and thus have a different size limit (125 vs. 20 μm) leading to different results. Moreover, different units for suspended (numbers per water volume) and settled MPs (numbers per sediment mass) impede direct comparisons. In this study, we overcome this limitation by recalculated MP sediment concentration (from this as well as previous publications, see Fig. 6) based on the average sediment density found in the Elbe. Although this approach is also associated with uncertainties, it is a relevant new approach to allow a broader comparison of global trends (Fig. 6).

Previous studies on global plastic pollution by Lebreton et al. (2017), Adam et al. (2018) and Besseling et al. (2018) pointed towards Asia as a key source of plastic pollution in aquatic ecosystems. In fact, many of the highest observed MP concentrations in water and sediment samples originate from Asian sampling sites. However, European sites (including the Elbe, especially in regard to its MP sediment concentrations) reach almost comparable levels (Fig. 6). High MP pollution is thus not exclusively restricted to the Asian countries or a single continent but is of global relevance.

5. Conclusion

This study provides for the first time data on MP pollution in the large European river Elbe and focused on the comparison of MPs in the water and sediment phase. MP concentrations were in average 600,000-fold higher in sediments (mean: $3.35 \times 10^6\ \text{p m}^{-3}$) compared to the water phase (mean: $5.57\ \text{p m}^{-3}$). PE and PP were the most common polymer types in the water phase, while in the sediments a more diverse polymer distribution was observed. Riverine sediments are, therefore, a key sink of MP pollution.

Besides differences between the water and sediment, MP concentrations varied also over the course of the river. Decreasing downstream concentrations, especially in the Elbe sediments, can be explained by a barrage dividing the Elbe in a section without (Middle Elbe) and with (Lower and Outer Elbe) tidal influence. Limit tidal activity above the barrage leads to the retention of the sediments in the Middle Elbe causing elevated MP concentrations.

In regard to MP sources, industrial activities seem to be of special relevance for the river Elbe. Industrial emissions near the city of Dessau probably cause local pollution hotspots with PS-DVB spheres. In contrary, no distinctive relation between urban surrounding and MP levels was found.

In a global context, MP concentrations in the Elbe water and sediments range in the lower (water) and medium (sediment) section of the global MP concentration range for river water and sediments. Especially elevated MP concentrations in sediments at some of the Elbe sampling sites illustrate well that MP pollution is not restricted to specific countries or continent, but it must be considered a global issue we need to approach.

CRedit authorship contribution statement

Christian Scherer: Conceptualization, Methodology, Investigation, Formal analysis, Writing - original draft, Writing - review & editing, Visualization, Validation. **Annikatrin Weber:** Investigation, Formal analysis, Writing - original draft, Writing - review & editing, Visualization. **Friederike Stock:** Investigation, Formal analysis, Writing - original draft, Writing - review & editing. **Sebastijan Vurusic:** Methodology, Investigation, Validation. **Harun Egerci:** Investigation, Validation. **Christian Kochleus:** Methodology, Investigation, Validation. **Niklas Arendt:** Investigation. **Corinna Foeldi:** Methodology, Investigation, Formal Analysis, Writing - original draft, Writing - review & editing, Validation. **Georg Dierkes:** Methodology, Investigation, Formal Analysis, Writing - original draft, Writing - review & editing, Validation. **Martin Wagner:** Conceptualization, Writing - review & editing, Supervision. **Nicole Brennholt:** Conceptualization, Writing - review & editing, Funding acquisition, Project administration. **Georg Reifferscheid:** Conceptualization, Writing - review & editing, Supervision.

Declaration of competing interest

The authors declare that they have no known competing financial interests or personal relationships that could have appeared to influence the work reported in this paper.

Acknowledgements

We appreciate the support of Prof. Dr. Jörg Oehlmann throughout the planning and performance of the sediment analyses at Goethe University. We further thank Anastasia Swonkow for her support throughout the validation of the sediment extraction method. Furthermore, we thank Prof. Dr. Michael Göbel and his research group for enabling and supporting the ATR-FTIR analysis and Lars Schumann for helping with GIS. The sampling was conducted by Julia Bachtin, Angela Koppers, Christel Möhlenkamp, Ramona Pfänder, Mandy Hoyer and Uwe Hentschke.

This study was funded by the German Federal Ministry of Transport and Digital Infrastructure.

Appendix A. Supplementary data

Supplementary data to this article can be found online at <https://doi.org/10.1016/j.scitotenv.2020.139866>.

References

- Adam, V., Yang, T., Nowack, B., 2018. Toward an ecotoxicological risk assessment of microplastics: comparison of available hazard and exposure data in freshwater. *Environ. Toxicol. Chem.* 38 (2), 436–447. <https://doi.org/10.1002/etc.4323>.
- Bagaev, A., Mazyuk, A., Khatmullina, L., Isachenko, I., Chubarenko, I., 2017. Anthropogenic fibres in the Baltic Sea water column: field data, laboratory and numerical testing of their motion. *Sci. Total Environ.* 599–600 (1), 560–571. <https://doi.org/10.1016/j.scitotenv.2017.04.185>.
- Bergmann, M., Gutow, L., Klages, M. (Eds.), 2015. *Marine Anthropogenic Litter*. Springer International Publishing, Cham, Heidelberg, New York, Dordrecht, London.
- Besseling, E., Redondo-Hasselrath, P., Foekema, E.M., Koelmans, A.A., 2018. Quantifying ecological risks of aquatic micro- and nanoplastic. *Crit. Rev. Environ. Sci. Technol.* 49 (1), 32–80. <https://doi.org/10.1080/10643389.2018.1531688>.
- Blair, R.M., Waldron, S., Phoenix, V.R., Gauchotte-Lindsay, C., 2019. Microscopy and elemental analysis characterisation of microplastics in sediment of a freshwater urban river in Scotland, UK. *Environ. Sci. Pollut. Res.* 26 (12), 12491–12504. <https://doi.org/10.1007/s11356-019-04678-1>.
- Brady, J., Dürig, T., Lee, P.I., Li, J.-X., 2017. Chapter 7-Polymer properties and characterization. In: Qiu, Y., Chen, Y., Zhang, G.G.Z., Yu, L., Mantri, R.V. (Eds.), *Developing Solid Oral Dosage Forms: Pharmaceutical Theory and Practice*, 2nd edition Academic Press, Burlington, London, San Diego, New York.
- Carpenter, E.J., Anderson, S.J., Harvey, G.R., Miklas, H.P., Peck, B.B., 1972. Polystyrene spherules in coastal waters. *Science* 178, 749–750. <https://doi.org/10.1126/science.178.4062.749>.

- Castañeda, R.A., Avlijas, S., Simard, M.A., Ricciardi, A., 2014. Microplastic pollution in St. Lawrence River sediments. *Can. J. Fish. Aquat. Sci.* 71 (12), 1761–1771. <https://doi.org/10.1139/cjfas-2014-0281>.
- Chubarenko, I., Bagaev, A., Zobjkov, M., Esiukova, E., 2016. On some physical and dynamical properties of microplastic particles in marine environment. *Mar. Pollut. Bull.* 108, 105–112. <https://doi.org/10.1016/j.marpolbul.2016.04.048>.
- Cole, M., Lindeque, P., Halsband, C., Galloway, T.S., 2011. Microplastics as contaminants in the marine environment: a review. *Mar. Pollut. Bull.* 62, 2588–2597. <https://doi.org/10.1016/j.marpolbul.2011.09.025>.
- Corcoran, P.L., 2015. Benthic plastic debris in marine and fresh water environments. *Environmental Science: Processes & Impacts* 17, 1363–1369. <https://doi.org/10.1039/C5EM00188A>.
- Dierkes, G., Lauschke, T., Becher, S., Schumacher, H., Földi, C., Ternes, T., 2019. Quantification of microplastics in environmental samples via pressurized liquid extraction and pyrolysis-gas chromatography. *Anal. Bioanal. Chem.* 411 (26), 6959–6968. <https://doi.org/10.1007/s00216-019-02066-9>.
- Dris, R., Gasperi, J., Rocher, V., Saad, M., Renault, N., Tassin, B., 2015a. Microplastic contamination in an urban area: a case study in Greater Paris. *Environ. Chem.* 12 (5), 592–599. <https://doi.org/10.1071/EN14167>.
- Dris, R., Imhof, H., Sanchez, W., Gasperi, J., Galgani, F., Tassin, B., Laforsch, C., 2015b. Beyond the ocean: contamination of freshwater ecosystems with (micro-) plastic particles. *Environ. Chem.* 12 (5), 539–550. <https://doi.org/10.1071/EN14172>.
- Duis, K., Coors, A., 2016. Microplastics in the aquatic and terrestrial environment: sources (with a specific focus on personal care products), fate and effects. *Environ. Sci. Eur.* 28 (2), 1–25. <https://doi.org/10.1186/s12302-015-0069-y>.
- Ehlers, S.M., Manz, W., Koop, J.H.E., 2019. Microplastics of different characteristics are incorporated into the larval cases of the freshwater caddisfly *Lepidostoma basale*. *Aquat. Biol.* 28, 67–77. <https://doi.org/10.3354/ab00711>.
- Eisentraut, P., Dümichen, E., Ruhl, A.S., Jekel, M., Albrecht, M., Gehde, M., Braun, U., 2018. Two birds with one stone—fast and simultaneous analysis of microplastics: microparticles derived from thermoplastics and tire wear. *Environmental Science & Technology Letters* 5, 608–613. <https://doi.org/10.1021/acs.estlett.8b00446>.
- Elbe, F.G.G., 2014. Aktualisierung der wirtschaftlichen Analyse (WA) der Wassernutzungen für die FGG Elbe. Abschlussbericht, 1–102. <https://publikationen.fgg-elbe.de/bewirtschaftungsplan/inhaltsverzeichnis.html>.
- Faure, F., Demars, C., Wieser, O., Kunz, M., de Alencastro, L.F., 2015. Plastic pollution in Swiss surface waters: nature and concentrations, interaction with pollutants. *Environ. Chem.* 12 (5), 582–591. <https://doi.org/10.1071/EN14218>.
- Fischer, M., Scholz-Böttcher, B.M., 2019. Microplastics analysis in environmental samples – recent pyrolysis-gas chromatography-mass spectrometry method improvements to increase the reliability of mass-related data. *Anal. Methods* 11, 2489–2497. <https://doi.org/10.1039/c9ay00600a>.
- Han, M., Niu, X., Tang, M., Zhang, B.-T., Wang, G., Yue, W., Kong, X., Zhu, J., 2019. Distribution of microplastics in surface water of the lower Yellow River near estuary. *Sci. Total Environ.* 707, 135601. <https://doi.org/10.1016/j.scitotenv.2019.135601>.
- Heß, M., Diehl, P., Mayer, J., Rehm, H., Reifenhäuser, W., Stark, J., Schweiger, J., 2018. Mikroplastik in Binnengewässern Süd- und Westdeutschlands Bundesländerübergreifende Untersuchungen in Baden-Württemberg, Bayern, Hessen, Nordrhein-Westfalen und Rheinland-Pfalz. Teil 1: Kunststoffpartikel in der oberflächennahen Wasserphase. Karlsruhe, Augsburg, Wiesbaden, Recklinghausen, Mainz. Online available. https://www.lanuv.nrw.de/fileadmin/lanuvpubl/6_sonderreihen/L%C3%A4nderbericht_Mikroplastik_in_Binnengew%C3%A4ssern.pdf (last access: May, 27th 2020).
- Hidalgo-Ruz, V., Gutow, L., Thompson, R.C., Thiel, M., 2012. Microplastics in the marine environment: a review of the methods used for identification and quantification. *Environmental Science & Technology* 46, 3060–3075. <https://doi.org/10.1021/es2031505>.
- Horton, A.A., Svendsen, C., Williams, R.J., Spurgeon, D.J., Lahive, E., 2017. Large microplastic particles in sediments of tributaries of the River Thames, UK – abundance, sources and methods for effective quantification. *Mar. Pollut. Bull.* 114 (1), 218–226. <https://doi.org/10.1016/j.marpolbul.2016.09.004>.
- Hurley, R., Woodward, J., Rothwell, J.J., 2018. Microplastic contamination of river beds significantly reduced by catchment-wide flooding. *Nat. Geosci.* 11, 251–257. <https://doi.org/10.1038/s41561-018-0080-1>.
- Imhof, H.K., Schmid, J., Niessner, R., Ivleva, N.P., Laforsch, C., 2012. A novel, highly efficient method for the separation and quantification of plastic particles in sediments of aquatic environments. *Limnology and Oceanography-Methods* 10, 524–537. <https://doi.org/10.4319/lom.2012.10.524>.
- Internationale Kommission zum Schutz der Elbe (IKSE, eds.), 2014. *Sedimentmanagementkonzept der IKSE, Vorschläge für eine gute Sedimentmanagementpraxis im Elbegebiet zur Erreichung überregionaler Handlungsziele*. Magdeburg, Germany. Online available. https://www.ikse-mkol.org/fileadmin/media/user_upload/D/06_Publikationen/01_Wasserrahmenrichtlinie/2014_IKSE-Abschlussbericht%20Sediment.pdf (last access: May 27th, 2020).
- Khatmullina, L., Isachenko, I., 2017. Settling velocity of microplastic particles of regular shapes. *Mar. Pollut. Bull.* 114, 871–880. <https://doi.org/10.1016/j.marpolbul.2016.11.024>.
- Klein, S., Worch, E., Knepper, T.P., 2015. Occurrence and spatial distribution of microplastics in river shore sediments of the Rhine-Main area in Germany. *Environmental Science & Technology* 49 (10), 6070–6076. <https://doi.org/10.1021/acs.est.5b00492>.
- Lahens, L., Strady, E., Kieu-Le, T.-C., Dris, R., Boukerma, K., Rinnert, E., Gasperi, J., Tassin, B., 2018. Macroplastic and microplastic contamination assessment of a tropical river (Saigon River, Vietnam) transversed by a developing megacity. *Environ. Pollut. Bull.* 661–671. <https://doi.org/10.1016/j.envpol.2018.02.005>.

- Lebreton, L.C.M., Van der Zwet, J., Damsteeg, J.-W., Slat, B., Andrady, A., Reisser, J., 2017. River plastic emissions to the world's oceans. *Nat. Commun.* 8, 15611. <https://doi.org/10.1038/ncomms15611>.
- Lechner, A., Keckeis, H., Lumesberger-Loisl, F., Zens, B., Krusch, R., Tritthart, M., Glas, M., Schludermann, E., 2014. The Danube so colourful: a potpourri of plastic litter outnumbers fish larvae in Europe's second largest river. *Environ. Pollut.* 188, 177–181. <https://doi.org/10.1016/j.envpol.2014.02.006>.
- Leslie, H.A., Brandsma, S.H., van Velzen, M.J.M., Vethaak, A.D., 2017. Microplastics en route: field measurements in the Dutch river delta and Amsterdam canals, wastewater treatment plants, North Sea sediments and biota. *Environ. Int.* 101, 133–142. <https://doi.org/10.1016/j.envint.2017.01.018>.
- Lin, L., Zuo, L.-Z., Peng, J.-P., Cai, L.-Q., Fok, L., Yan, Y., Li, H.-X., Xu, X.-R., 2018. Occurrence and distribution of microplastics in an urban river: a case study in the Pearl River along Guangzhou City, China. *Sci. Total Environ.* 644, 375–381. <https://doi.org/10.1016/j.scitotenv.2018.06.327>.
- Loeder, M.G.J., Gerdt, G., 2015. Methodology used for the detection and identification of microplastics—a critical appraisal. In: Bergmann, M., Gutow, L., Klages, M. (Eds.), *Marine Anthropogenic Litter*. Springer International Publishing, Cham.
- Mai, L., Bao, L.-J., Shi, L., Wong, C.S., Zeng, E.Y., 2018. A review of methods for measuring microplastics in aquatic environments. *Environ. Sci. Pollut. Res.* 25, 11319–11332. <https://doi.org/10.1007/s11356-018-1692-0>.
- Mani, T., Hauk, A., Walter, U., Burkhardt-Holm, P., 2015. Microplastics profile along the Rhine River. *Sci. Rep.* 5, 17988. <https://doi.org/10.1038/srep17988>.
- Mani, T., Blarer, P., Storck, F.R., Pittroff, M., Wernicke, T., Burkhardt-Holm, P., 2019. Repeated detection of polystyrene microbeads in the lower Rhine River. *Environ. Pollut.* 245, 634–641. <https://doi.org/10.1016/j.envpol.2018.11.036>.
- Moret-Ferguson, S., Law, K.L., Proskurowski, G., Murphy, E.K., Peacock, E.E., Reddy, C.M., 2010. The size, mass, and composition of plastic debris in the western North Atlantic Ocean. *Mar. Pollut. Bull.* 60, 1873–1878. <https://doi.org/10.1016/j.marpolbul.2010.07.020>.
- Naumann, S., Schriever, S., Möhling, M., Hansen, O., 2003. Bedeutung der Nebenflüsse für den Feststoffhaushalt der Elbe. Final report. BfG-1382. Federal Institute of Hydrology, Koblenz.
- Norén, F., 2007. *Small plastic particles in coastal Swedish waters*. Report by Kommunenes Internasjonale Miljøorganisasjon. Online available. <http://www.n-research.se/pdf/Small%20plastic%20particles%20in%20Swedish%20West%20Coast%20Waters.pdf> (last access: May 27th, 2020).
- PlasticsEurope, 2017. *Plastics - the facts 2017: an analysis of European plastics production, demand and waste data*. Online. https://www.plasticseurope.org/application/files/5715/1717/4180/Plastics_the_facts_2017_FINAL_for_website_one_page.pdf.
- Prata, J.C., da Costa, J.P., Duarte, A.C., Rocha-Santos, T., 2019. Methods for sampling and detection of microplastics in water and sediments: a critical review. *Trends Anal. Chem.* 110, 150–159. <https://doi.org/10.1016/j.trac.2018.10.029>.
- Rodrigues, M.O., Abrantes, N., Gonçalves, F.J.M., Nogueira, H., Marques, J.C., Gonçalves, A.M.M., 2018. Spatial and temporal distribution of microplastics in water and sediments of a freshwater system (Antuã River, Portugal). *Sci. Total Environ.* 633, 1549–1559. <https://doi.org/10.1016/j.scitotenv.2018.03.233>.
- Rodrigues, S.M., Almeida, C.M.R., Silva, D., Cunha, J., Antunes, C., Freitas, V., Ramos, S., 2019. Microplastic contamination in an urban estuary: abundance and distribution of microplastics and fish larvae in the Douro estuary. *Sci. Total Environ.* 659, 1071–1081. <https://doi.org/10.1016/j.scitotenv.2018.12.273>.
- Schmidt, L.K., Bochow, M., Imhof, H.K., Oswald, S.E., 2018. Multi-temporal surveys for microplastic particles enabled by a novel and fast application of SWIR imaging spectroscopy - study of an urban watercourse traversing the city of Berlin, Germany. *Environ. Pollut.* 239, 579–589. <https://doi.org/10.1016/j.envpol.2018.03.097>.
- Schwartz, R., Eichweber, G., Entelmann, I., Keller, I., Rickert-Niebuhr, K., Röper, H., Wenzel, C., 2015. Aspekte des Schadstoff-Sedimentmanagements im Bereich der Tideelbe. Aspects of pollutant sediment management in the tidal Elbe. *Fachzeitschrift für Hydrologie und Wasserbewirtschaftung* 59 (6), 414–426. https://doi.org/10.5675/HyWa_2015.6.9.
- Tibbetts, J., Krause, S., Lynch, I., Smith, G.H.S., 2018. Abundance, distribution, and drivers of microplastic contamination in urban river environments. *Water* 10, 1597. <https://doi.org/10.3390/w10111597>.
- Unice, K.M., Kreider, M.L., Panko, J.M., 2012. Use of a deuterated internal standard with pyrolysis-GC/MS dimeric marker analysis to quantify tire tread particles in the environment. *Int. J. Environ. Res. Public Health* 9, 4033–4055. <https://doi.org/10.3390/ijerph9114033>.
- Wagner, M., Lambert, S. (Eds.), 2018. *Freshwater Microplastics: Emerging Environmental Contaminants*? Springer International Publishing, Cham, Heidelberg, New York, Dordrecht, London.
- Waldschläger, K., Schuettrumpf, H., 2019. Effects of particle properties on the settling and rise velocities of microplastics in freshwater under laboratory conditions. *Environmental Science & Technology* 53, 1958–1966. <https://doi.org/10.1021/acs.est.8b06794>.
- Wang, W., Ndungu, A.W., Li, Z., Wang, J., 2017b. Microplastics pollution in inland freshwaters of China: a case study in urban surface waters of Wuhan, China. *Sci. Total Environ.* 575, 1369–1374. <https://doi.org/10.1016/j.scitotenv.2016.09.213>.
- Wang, Z., Su, B., Xu, X., Di, D., Huang, H., Mei, K., Dahlgren, R.A., Zhang, M., Shang, X., 2018. Preferential accumulation of small (<300 μm) microplastics in the sediments of a coastal plain river network in eastern China. *Water Res.* 144, 393–401. <https://doi.org/10.1016/j.watres.2018.07.050>.
- Wolanski, E., Elliott, M., 2015. *Estuarine Ecohydrology: An Introduction*. 2nd edition. Elsevier Science, Amsterdam, Oxford.
- Xiong, X., Wu, C., Elser, J.J., Mei, Z., Hao, Y., 2019. Occurrence and fate of microplastic debris in middle and lower reaches of the Yangtze River – from inland to the sea. *Sci. Total Environ.* 659, 66–73. <https://doi.org/10.1016/j.scitotenv.2018.12.313>.